The 2010 IEEE/RSJ International Conference on
Intelligent Robots and Systems
October 18-22, 2010, Taipei, Taiwan

Construction of a compact range image sensor using multi-slit laser projector and obstacle detection of a humanoid with the sensor

Takahiro Kuroki, Kenji Terabayashi and Kazunori Umeda

Abstract— **Detection of obstacles on a plane is important for a mobile robot that moves in a living space, especially for a humanoid that falls down even with a small obstacle. In this paper, a range image sensor for detecting small obstacles on a plane is constructed using a multi-slit laser projector. The sensor consists of a commercially available laser projector and a CCD camera. It measures a relative disparity map (RDMap) whose measurement errors are not affected by the distance. From the obtained RDMap, a plane is estimated using RANSAC and regions out of the plane are detected as obstacles. Experiments show that planes can be obtained with small errors in RDMaps with the constructed sensor, and that a humanoid with the constructed sensor can detect small obstacles such as a moving ping-pong ball and a LAN cable on a plane by the proposed methods while walking.**

I. INTRODUCTION

Robots are currently being used in human environments, such as offices and houses. Because there are many obstacles in these environments, a robot must be able to detect planar regions in which it can move [1], [2]. For this purpose, three-dimensional (3D) information is necessary, and range images are effective as the 3D information. Many methods to acquire range images have been studied. For robot applications, real-time sensing is necessary, and some of the methods can achieve real-time range imaging. Stereo vision is very common and commercial sensors are available [3]. However, stereo vision has an essential problem, i.e., stereo correspondence problem [4]. In [5], a 3D map is reconstructed using stereo vision and a humanoid can walk through a room full of objects to reach its goal in the experiment. However, the stereo correspondence problem is avoided by putting artificial patterns on most of the obstacles.

On the other hand, active sensors can obtain 3D information of an environment more robustly without the correspondence problem. Beraldin et al. achieved video-rate range imaging by scanning a laser spot using their synchronized laser scan technique [6]. Kanade [7] developed a special imaging detector and achieved real-time imaging by scanning a laser slit with the detector. Nakazawa [8] constructed a sensor without scanning by projecting multi-spots. The spot pattern was generated using a fiber grating and a laser. We also constructed a range image sensor using a multi-spot laser projector [9], [10]. This sensor has been used for a humanoid, and the humanoid can detect obstacles on a plane while walking [11]. However, the sensor using a multi-spot laser sometimes fails to detect obstacles that are smaller or thinner than the intervals of the projected spots. Kawai et al. [12] considered that a light slit is the aggregate of light spots and achieved high density of measurement.

In this paper, we construct a range image sensor using a multi-slit laser projector. The sensor can measure a range image that is denser than the one obtained by the sensor with a multi-spot projector. A range image can be obtained with one image in real time, without scanning. We apply this sensor to detect small obstacles. For this purpose, the sensor measures a relative disparity map (RDMap)[9], [11]. Marton et al.[13] extracted objects on a table by estimating model of the plane using RANSAC [14]. We apply similar estimation to an RDMap. A plane is estimated and regions out of the plane are detected as obstacles.

This paper is organized as follows. Firstly, the constructed sensor is described. Next, the method to detect obstacles is introduced as the application of the sensor. Experiments to measure RDMaps for different pose parameters are shown. Finally, experiments verify that a humanoid with the sensor can detect small obstacles on a plane using the proposed method while walking and avoid the obstacles.

II. RANGE IMAGE SENSOR USING A MULTI-SLIT LASER PROJECTOR

A. Principle of the sensor

Fig.1 illustrates the structure of the sensor. Multiple laser slits are projected by a laser projector, and a scene with projected multi-slits are observed by a CCD camera. The slits in images of the CCD camera are extracted, and for each point of each slit, disparity can be measured and distance is calculated by the simple triangulation. In this sensor, the correspondence problem occurs; as there are multiple slits, it is necessary to obtain the correspondence between projected slits and their observed images. In this paper, we take the practical method: limiting measurement range so that the correspondences become unique.

We rotate the CCD camera to increase the measurement range [9]. Fig.2(a) illustrates the image of slits without rotating the camera. In the image plane, each point on each slit moves along the epipolar line according to the distance. So as to achieve the uniqueness of the correspondence, movable ranges of slits in the image have to be restricted so that they have no overlap as shown in Fig.2(a). This limit can be relaxed by rotating the CCD camera as shown in Fig.3. Fig.2(b) illustrates the image of slits with the rotation. This

T. Kuroki is with the Course of Precision Engineering, School of Science and Engineering, Chuo University, 1-13-27 Kasuga, Bunkyo-ku, Tokyo 112-8551, Japan kuroki@sensor.mech.chuo-u.ac.jp

K. Terabayashi and K. Umeda are with Department of Precision Mechanics, Faculty of Science and Engineering, Chuo University, 1-13-27 Kasuga, Bunkyo-ku, Tokyo 112-8551, Japan {terabayashi,umeda}@mech.chuo-u.ac.jp

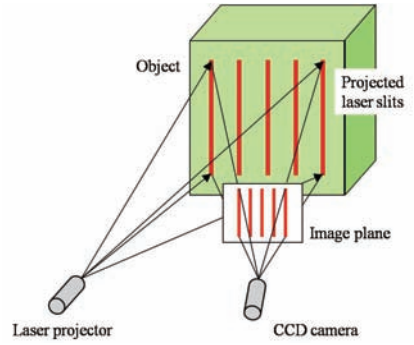

Fig. 1. Structure of the range image sensor using a multi-slit laser projector

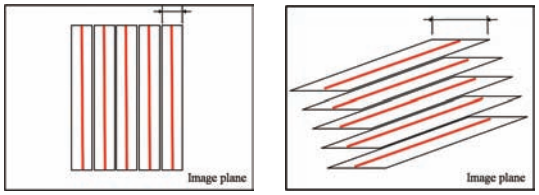

(a) Without rotation (b) With rotation

Fig. 2. Restriction for epipolar line of each slit

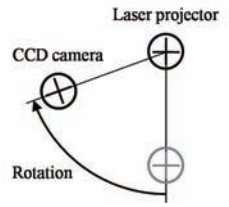

Fig. 3. Rotation of CCD camera to increase measurement range

figure shows that the movable ranges of slits become larger. Consequently, the measurable range of the sensor becomes larger, or with the same measurable range, the precision of measurement can be improved because the number of the assigned pixels for measuring the same range becomes larger. When the rotation angle is θ, the movable range of a slit becomes $1/cos\theta$ times. There is a trade-off, though: the vertical length of the slit becomes $cos\theta$ times, which reduces the number of points of a range image. Since the resolution of the range image with the sensor is anisotropic: much higher along the slit, we think the trade-off should be taken.

B. Sensor hardware

Fig.4 shows the constructed range image sensor.

The laser projector is StockerYale Mini-715L [15]. The wavelength of the laser is 660nm and its power is 35mW. It projects 15 slits. The angle between adjacent slits is 2.3°.

The CCD camera is Point Grey Research Flea2. The number of pixels is 1296×964, and the size of the pixel is $3.75\times3.75\mu m^2$. A lens with f=4mm is used, and a Kenko R64 optical filter is attached to the lens. With the optical filter, lights under 640nm are cut, which improves the S/N ratio of the slit image. The camera is connected to a PC and

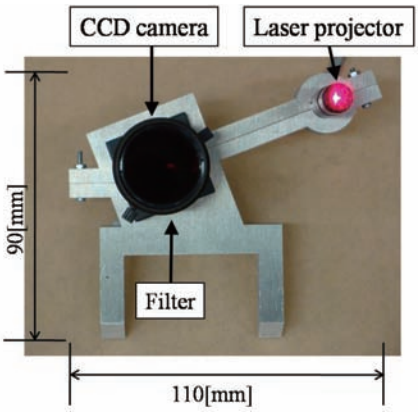

Fig. 4. Constructed compact range image sensor

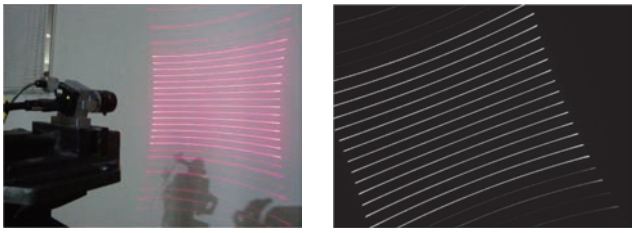

(a) Projected laser slits (b) CCD image for (a)

Fig. 5. Projected laser slits and corresponding image

the image captured by the camera is processed with the PC.

The baseline length between the laser projector and the CCD camera is 60mm. The CCD camera is rotated by 70°. Consequently, the number of pixels assigned to each slit increases from 22 to 55. The number of points of obtained range image is 4938, which means that about 330 points are measured for each of 15 slits. And it is much more than that of the former sensor 361 (19×19) with a multi-spot projector[9], [10]. Field of view of the sensor (not the CCD camera) is 45°×32°.

Fig.5 shows the projected laser slits and corresponding image obtained by the CCD camera. We can see the large rotation of the slits in Fig.5(b). Additionally, large distortion of the projected slits is observed. This is the specification of the laser projector and unavoidable (probably because of large field of view). With this distortion, the assigned pixels decreases; 22 pixels / $cos70°$ is 64 pixels, but it is suppressed to 55 pixels as described above.

C. Initial setting of the sensor

For initial setting, we set the sensor in front of a vertical plane with the optical axis parallel to the normal of the plane as shown in Fig.5(a). Then we use the obtained image Fig.5(b) as the reference image of multi-slits to set the reference position of each point on each slit. The sensor is constructed to have the parallel stereo configuration. Therefore the epipolar line is horizontal in image. An obtained image is scanned horizontally at every row of the image as shown in Fig.6, and the centroids of a slit are calculated along the horizontal direction. The centroid is used as the

Fig. 6. Magnified image of Fig.5(b)

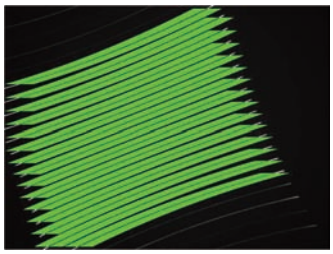

(a) Assigned regions to measure disparity for Fig.5(b)

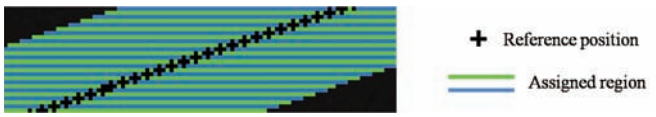

(b) Magnified image of (a). Regions are colored row by row alternately for visibility.

Fig. 7. Assigned regions to measure disparity

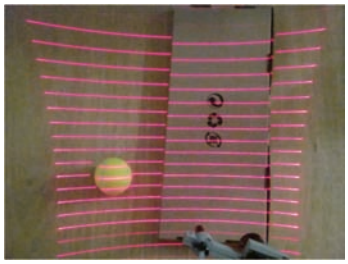

(a) Target scene

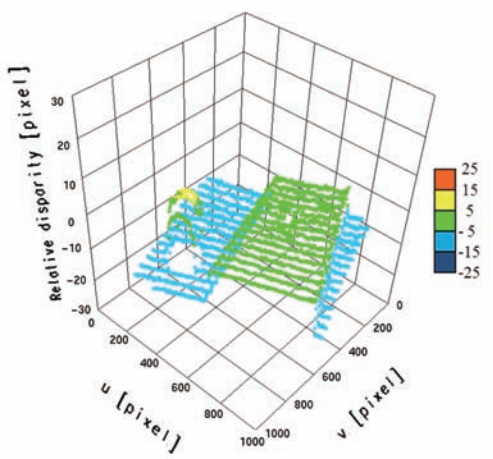

(b) Obtained RDMap

Fig. 8. An example of RDMap

reference point. Fig.7 shows the calculated centroids and regions assigned to each point on each slit. As mentioned above, the regions are assigned so that they have no overlap. The width of the assigned regions is kept constant (i.e., 55 pixels) for every point. The sensor searches the slit in the assigned region and obtains disparity.

III. DETECTION OF OBSTACLES USING A RELATIVE DISPARITY MAP

For mobile robots including humanoids, it is necessary to find their movable regions in real time. Therefore, detection of planar regions on which they can move is necessary. We have proposed an RDMap as a suitable representation of scene for this purpose. In this section, we propose a method to detect planar regions and regions of obstacles using RDMaps with the constructed range image sensor.

A. Measurement of a relative disparity map[9], [11]

An RDMap is defined as follows. A range image sensor observes a reference plane in advance. And when the sensor observes a target scene, it detects a relative disparity for the reference plane at each point. We call the set of the relative disparities as an RDMap. In an RDMap, a plane in the real 3D space also becomes a plane. Therefore, it is possible to detect planar regions in the map. In addition, an RDMap has a feature that measurement errors are not affected by the distance. This feature is suitable for robust detection of planar regions when the pose of the sensor and the distance to the target changes significantly.

Fig.8 shows an example of measurement of an RDMap using the constructed sensor. In advance, the sensor observed the wooden floor as a reference plane. Then a tennis ball of about 70 mm in diameter and a 185mm×455mm×30mm box were set as shown in Fig.8(a), and the scene was measured from the 50mm higher position. Fig.8(b) shows the obtained RDMap. u and v indicate the reference position of each point of slits in the image. We can see that the floor keeps planar in the RDMap, and the disparities at the ball and the box are out of the plane.

B. Detection of obstacles

We propose a method to detect obstacle regions on a plane in an RDMap. We use RANSAC[14] to detect a plane in an RDMap. RANSAC can estimate model parameters robustly from measured data with outliers. With the estimated plane parameters, planar regions and obstacle regions are separated.

A plane in an RDMap is given as

$$\Delta k = Au + Bv + C, \tag{1}$$

where A, B and C are parameters of the plane, u and v are the coordinate of centroid of points in slit, and Δk is the measured relative disparity.

RANSAC chooses three points at random in different slits and determines the plane parameters. Then the number of points that are regarded to belong to the plane is counted. The threshold to judge if the point belongs to the plane is decided empirically. This procedure is repeated in a certain number, and the case with the maximum count is chosen. Then a least-squares plane is obtained for the points that belong to the chosen plane. The parameters are calculated

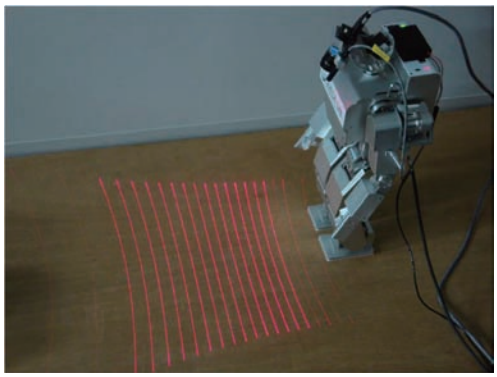

Fig. 9. Compact range image sensor and humanoid

by

$$\begin{Bmatrix} A \\ B \\ C \end{Bmatrix} = \begin{bmatrix} \sum u^2 & \sum uv & \sum u \\ \sum uv & \sum v^2 & \sum v \\ \sum u & \sum v & N \end{bmatrix}^{-1} \begin{Bmatrix} \sum u\Delta k \\ \sum v\Delta k \\ \sum \Delta k \end{Bmatrix}, \quad (2)$$

where N is used number of the chosen points. With the obtained least-squares plane, planar regions and obstacle regions are separated; the points that are apart from the plane are detected as obstacle regions. The threshold to judge if a point belong to a plane at RANSAC and final stages can be decided empirically.

By the way, the number of plane fitting at RANSAC can be decided statistically with the following equation.

$$P = 1 - \{1 - (1 - \epsilon)^F\}^q \quad (3)$$

P is the probability to choose a correct model, and ϵ is the ratio of outliers in the total measurement data. F is the number of data to determine the model, and q is the number of iterations. In the experiments, we set $P = 0.99$ and $\epsilon = 0.5$. $F = 3$, and consequently, $q = 35$ is obtained from (3).

C. Application to a humanoid

We apply the method of detecting obstacle regions to a walking humanoid. Fig.9 shows a humanoid Fujitsu HOAP-2 with the constructed sensor. The sensor is attached to be able to measure regions near the foot of the humanoid. The direction of the slits and the direction in which the humanoid walks are perpendicular. Therefore, the slits sweep the floor with respect to the motion of the humanoid, and thus even a small obstacle is not lost, which was the case with a multi-spot sensor.

IV. EXPERIMENTS TO EVALUATE MEASUEMENT OF RELATIVE DISPARITY MAP

In this section, we show experimental results to evaluate measurement of an RDMap with the constructed sensor. Fig.10 shows the pose parameters of the sensor for the floor. We measured an RDMap and fitted a plane to all measured points using (2), and evaluated the standard deviation of the residual of each point for the fitted plane. RDMaps were measured under various pose parameters as shown in Table I. One of the three parameters is changed from the reference pose that corresponds to the initial pose of the humanoid.

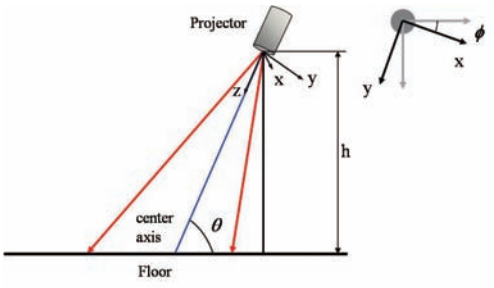

Fig. 10. Pose parameters of range image sensor

TABLE I
EXPERIMENRTAL CONDITIONS FOR PLANE FITTING

Condition	θ [deg]	ϕ [deg]	h [mm]
Reference	66	0	445
1	61	0	445
2	71	0	445
3	66	-5	445
4	66	5	445
5	66	0	395
6	66	0	495

Fig.11 shows examples of RDMaps for Condition 2, 4, 6. We can see that an RDMap of a plane keeps planar for various pose. Fig.12 shows the average of standard deviations of the residuals for each condition. 100 standard deviations were averaged. We can see from Fig.12 that the standard deviations are almost constant for different conditions. This is because the RDMap is not affected by the distance, which suggests that the proposed system is suitable for a mobile robot with changing pose such as a humanoid.

And from Fig.12, we set the uncertainty (standard deviation) of the measurement of relative disparity of the constructed sensor to 0.3 pixel. When RANSAC is applied, and planar and obstacle regions are separated, the threshold was set to 3σ, i.e., 0.9 pixel.

V. EXPERIMENTS OF OBSTACLE DETECTION BY A WALKING HUMANOID

We verified that a walking humanoid can detect small obstacles with the proposed sensor system by experiments. The humanoid's motion was as follows. If no obstacle is detected, the humanoid continues walking straightforward. If an obstacle is detected and it is not very near, the humanoid rotates until no obstacle is detected. And if an obstacle is suddenly detected at very near position, the humanoid stops for 5s.

To show that the sensor system can detect small or thin obstacles, we used a ping-pong ball with diameter 40mm and a LAN cable with diameter 7mm. The LAN cable was set in front of the humanoid, firstly out of the field of view of the sensor. The ball was thrown in just in front of the foot of the humanoid.

Fig.13 shows the experimental scenes. In each figure, green spots (not possible to see each spot, though) show the obtained RDMap and a light green plane show the extracted plane. When obstacles are detected, the regions are indicated

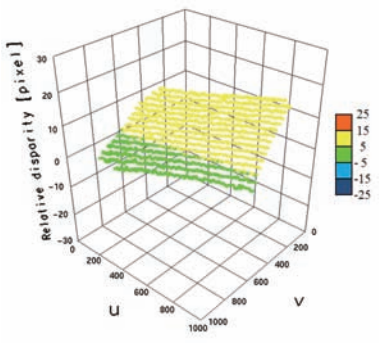

(a) Condition2

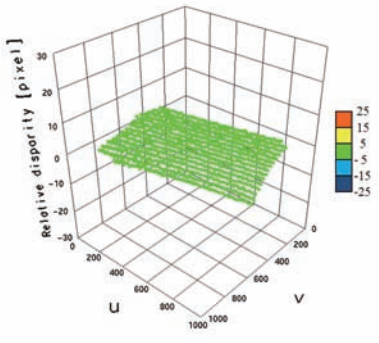

(b) Condition4

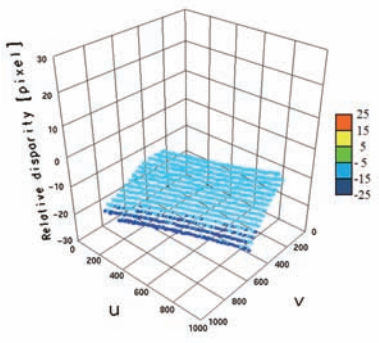

(c) Condition6

Fig. 11. RDMaps for several conditions

in red. Firstly, the walking humanoid could detect the ping-pong ball that appeared suddenly and stopped (Fig.13(c)). Then the humanoid resumed walking. The humanoid detected the LAN cable (Fig.13(i)), rotated leftward (Fig.13(j)-(l)), and resumed walking again. Fig.14 shows one of the RDMaps at around 20s. We can see that the plane and the LAN cable are detected appropriately. Fig.15 shows the number of points detected as the obstacle regions in the sequence of the experiment. The peak around frame 200 shows the detection of the ping-pong ball, and the data from 500-800 frames correspond to the detection of LAN cable. The sampling rate was more than 30Hz including the detection of obstacles. The accompanying video verifies the real-time obstacle detection.

From the experimental results, we can see that the humanoid can detect small or thin obstacles and avoid them with the constructed sensor and the proposed method to detect obstacles.

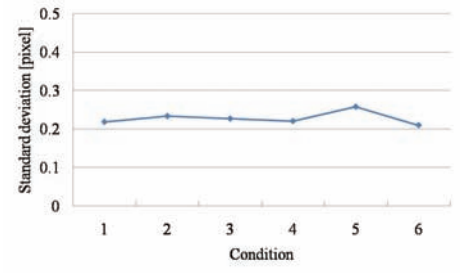

Fig. 12. Average of standard deviations of the residuals from fitted plane

VI. CONCLUSION

In this paper, we constructed a range image sensor using a multi-slit laser projector for detecting small obstacles on a plane. The sensor consists of a commercially available laser projector and a CCD camera. Relative disparity maps (RDMaps) were obtained as appropriate information for the purpose. A plane is estimated from an RDMap using RANSAC and regions out of the plane are detected as obstacles. It was shown that small obstacles such as a moving ping-pong ball and a LAN cable could be detected with a walking humanoid in real time. Compared to the former sensor that used a multi-spot projector, the constructed sensor is superior in that it can detect smaller or thinner obstacles.

The future works include detection of smaller obstacles such as small screws using sequential data, and precise error analysis of the constructed sensor and the system. Extension to measurement of range images with absolute scale with the sensor should also be done.

VII. ACKNOWLEDGMENTS

This work was supported by KAKENHI (20500164).

REFERENCES

[1] K. Okada, S. Kagami, M. Inaba, and H. Inoue, "Plane Segment Finder: Algorithm, Implementation and Applications," Proc. of International Conference on Robotics and Automation (ICRA'01), pp. 2120-2125, 2001.

[2] N. Pears and B. Liang, "Ground Plane Segmentation for Mobile Robot Visual Navigation," Proc. 2000 IEEE/RSJ International Conference on Intelligent Robots and System (IROS 2001), pp. 1513- 1518, 2001.

[3] For example, Point Grey Research Inc. http://www.ptgrey.com

[4] T. Kanade, "Development of a Video-Rate Stereo Machine," Proceedings of the 1994 ARPA Image Understanding Workshop (IUW'94), pp. 549-558, Nov., 1994.

[5] R. Ozawa, Y. Takaoka, Y. Kida, K. Nishiwaki, J. Chestnutt, J. Kuffner, J. Kagami, H. Mizoguch, and H. Inoue, "Using Visual Odometry to Create 3D Maps for Online Footstep Planning," Proceedings of IEEE International Conference on Systems, Man and Cybernetics (SMC2005), Hawaii, USA, pp. 2643-2648, Oct., 2005.

[6] J. A. Beraldin, F. Blais, M. Rioux, J. Domery, and L. Cournoyer, "A video rate laser range camera for electronic boards inspection," Proc. Vision'90 Conference, pp. 4-1-4-11, 1990.

[7] T. Kanade, A. Gruss, and L. R. Carley, "A VLSI sensor based range finding system," Robotics Research Fifth International Symposium, pp. 49-56, 1990.

[8] K. Nakazawa and C. Suzuki, "Development of 3-D robot vision sensor with fiver grating: Fusion of 2-D intensity image and discrete range image," Proc. 1991 International Conference on Industrial Electronics, Control and Instrumentation (IECON'91), pp. 2368- 2372, 1991.

[9] K. Umeda,"A Compact Range Image Sensor Suitable for Robots," Proc. 2004 Int. Conf. On Robotics and Automation, pp. 3167-3172, 2004.

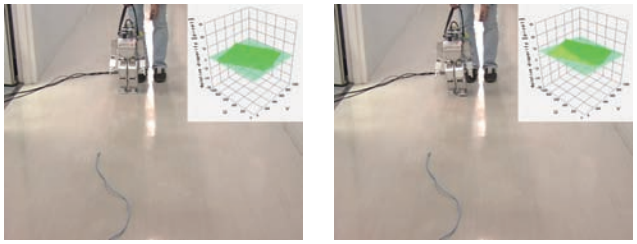

(a) 0s (b) 2s

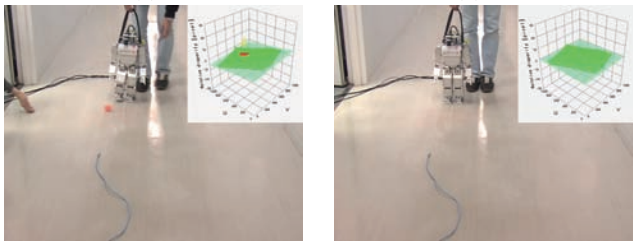

(c) 4s (d) 6s

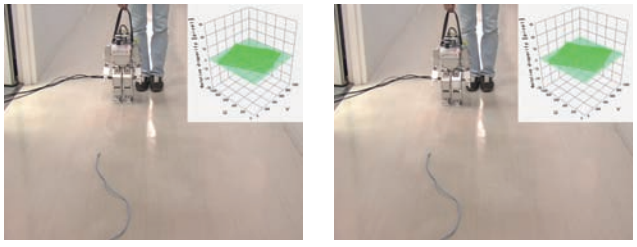

(e) 8s (f) 10s

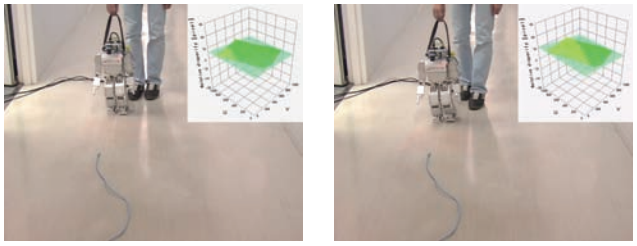

(g) 12s (h) 14s

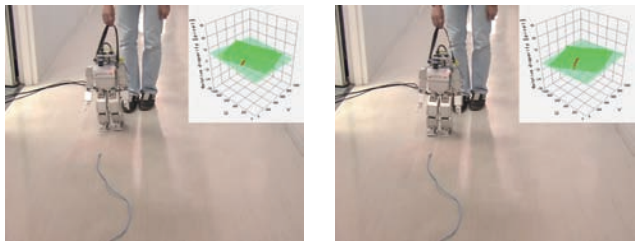

(i) 16s (j) 18s

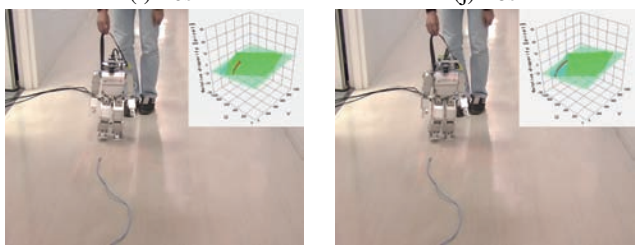

(k) 20s (l) 22s

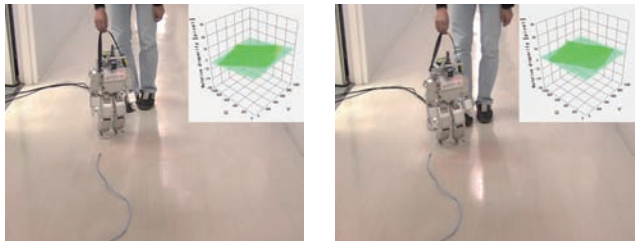

(m) 24s (n) 26s

Fig. 13. Experimental results of obstacle detection by walking humanoid

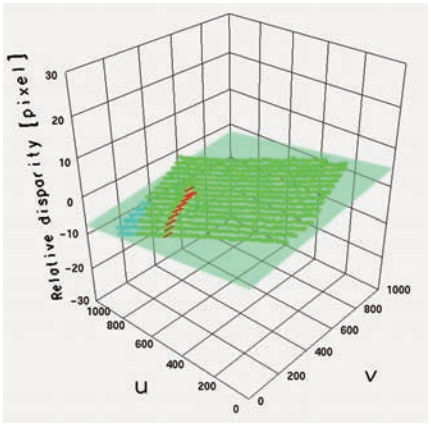

Fig. 14. An RDMap with the detected plane and an obstacle (LAN cable)

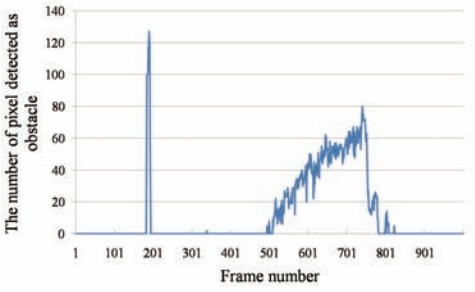

Fig. 15. The number of points detected as obstacles

[10] M. Tateishi, H. Ishiyama and K. Umeda, "A 200Hz Small Range Image Sensor Using a Multi-Spot Laser Projector," Proc. 2008 IEEE International Conference on Robotics and Automation, FrA9.6 A 3022, 2008.

[11] N. Hikosaka, K. Watanabe, and K. UMEDA, "Obstacle Detection of a Humanoid on a Plane Using a Relative Disparity Map Obtained by a Small Range Image Sensor," Proc. of IEEE International Conference on Robotics and Automation, pp.3048-3053, 2007.

[12] R. Kawai, A. Yamashita and T. Kaneko, "Three-dimensional measurement of objects in water by using space encoding method," Proc. 2009 IEEE International Conference on Robotics and Automation, pp. 1579-1584, 2009.

[13] Z. C. Marton, R. B. Rusu, D. Jain, U. Klank, and M. Beetz, "Probabilistic Categorization of Kitchen Objects in Table Settings with a Composite Sensor," Proc. 2009 IEEE/RSJ International Conference on Intelligent Robots and Systems, pp. 4777-4784, 2009.

[14] M. A. Fischler and R. C. Bolles, "Random Sample Consensus: A Paradigm for Model Fitting with Applications to Image Analysis and Automated Cartography," in Comm. of the ACM, Vol.24, No.6, 1981.

[15] StockerYale, Inc. http://www.stockeryale.com/